Radiomics Analysis Based on Optical Coherence Tomography to Prognose the Efficacy of Anti-VEGF Therapy of Retinal Vein Occlusion-Related Macular Edema

Biying Chen,[1,2] Jianing Qiu,[1,2] Yongan Meng,[1,2] Youling Liang,[1,2] Dan Liu,[1,2] Yuqian Hu,[1,2] Zhishang Meng,[1,2] and Jing Luo[1,2]

[1]Department of Ophthalmology, the Second Xiangya Hospital, Central South University, Changsha, Hunan Province, China
[2]Hunan Clinical Research Center of Ophthalmic Disease, Changsha, Hunan Province, China

Correspondence: Jing Luo, Department of Ophthalmology, the Second Xiangya Hospital of Central South University, 139 Middle Renmin Rd., Changsha, Hunan 410011, China; luojing001@csu.edu.cn.
Zhishang Meng, Department of Ophthalmology, the Second Xiangya Hospital of Central South University, 139 Middle Renmin Rd., Changsha, Hunan 410011, China; mengzhishang@csu.edu.cn.

BC and JQ contributed equally to this work.

Received: October 18, 2024
Accepted: March 23, 2025
Published: April 25, 2025

Citation: Chen B, Qiu J, Meng Y, et al. Radiomics analysis based on optical coherence tomography to prognose the efficacy of anti-VEGF therapy of retinal vein occlusion-related macular edema. *Invest Ophthalmol Vis Sci.* 2025;66(4):74. https://doi.org/10.1167/iovs.66.4.74

Purpose. Anti-vascular endothelial growth factor (anti-VEGF) agents are the first-line treatment for retinal vein occlusion-related macular edema (RVO-ME). However, the availability of reliable radiomic markers for evaluating the effectiveness of these agents is currently limited. The aim of this study was to develop machine learning approaches to evaluate the post-therapeutic effect of anti-VEGF treatment based on optical coherence tomography (OCT) images.

Methods. A total of 152 patients diagnosed with RVO-ME who received at least one intravitreal injection of anti-VEGF were included in this study, as well as 81 patients as the external validation set. Pre-therapeutic B-scans of spectral-domain OCT images were collected and segmented using the Pyradiomics module within the 3D Slicer software platform. Radiomic features were extracted from the segmented images. We trained the logistic regression model and machine learning models using the selected features, and evaluated the performance of the three classifier models.

Results. In the back propagation neural network (BPNN) model, the area under the curve (AUC) of the training, test, and external validation sets were 0.977, 0.912, and 0.804, respectively. In the support vector machine (SVM) model, the AUC of the 3 sets were 0.916, 0.882, and 0.802. The OCT-omics scores indicated a high overall net benefit, as determined by decision curve analysis.

Conclusions. The machine learning models based on OCT technology developed here demonstrated a promising ability to prognose anti-VEGF therapeutic responses for RVO-ME. The utilization of machine learning provides a new promising approach to assessing radiomic markers in research related to RVO-ME, having a good prospect for the application of the using of precision medicine in ophthalmology.

Keywords: machine learning, radiomics, optical coherence tomography (OCT), retinal vein occlusion-related macular edema (RVO-ME), anti-VEGF therapy

Retinal vein occlusion (RVO) has remained the second most common retinal vascular diseases after diabetic retinopathy, estimated to affect up to 16.4 million adults worldwide.[1] Macular edema (ME) and retinal ischemia are the main complications of RVO. In particular, ME is one of the most common reasons for vision loss in patients with RVO, resulting in disruption to patients' daily life activities and function.[2]

Vascular endothelial growth factor (VEGF) serves as a significant cytokine responsible for the mediation of increasing vascular permeability, consequently leading to macular edema.[3] Several studies have investigated the efficacy of anti-VEGF therapy in enhancing visual and anatomical outcomes.[4,5] However, a small proportion of patients with RVO-ME do not demonstrate improvement following anti-VEGF therapy.[5,6] In consideration of the high heterogeneity in drug efficacy and diversity of anti-VEGF drugs, even experienced clinicians have difficulty accurately predicting the effectiveness of anti-VEGF therapy for individual patients, which needs to develop a new approach for prognostication.

With the rapid development of imaging technology in ophthalmic medicine, optical coherence tomography (OCT) is widely used in ophthalmology, which allows for both qualitative identification and quantitative analysis of imaging markers.[7,8] In particular, OCT helps confirm the presence of ME and enables quantitative assessment of retinal thickening, and provides additional information, such as presence of vitreoretinal interface abnormalities, serous retinal detachment, and pigment epithelial changes that may further guide therapy.[9] Consequently, OCT severs as an important examination tool for the diagnosis and prognosis of macular disorders.[10] Simultaneously, radiomics is increasingly being recognized as a valuable technique for converting medical images, such as computed tomography (CT) or magnetic resonance imaging (MRI), into analyz-

able high-dimensional data.[11] It has been utilized in various medical domains, including the identification, prediction, and therapeutic decision making in tumor cases, as well as the screening for lumbar spine osteoporosis, and other medical fields.[12,13] In ophthalmology, researches based on radiomics and machine learning have successfully demonstrated the ability to predict anti-VEGF therapy response in patients with diabetic ME and age-related macular degeneration.[14]

Therefore, the objective of this study was to find a novel OCT radiomic marker capable of predicting the efficacy of anti-VEGF therapy for RVO-ME.

Methods

Ethics

This retrospective cohort study obtained ethical approval (no. 2017-053) from the Ethics Committee of the Second Xiangya Hospital, Central South University, in accordance with the Declaration of Helsinki and other ethical guidelines. To ensure privacy and comply with data protection regulations, all patient data were anonymized and treated confidentially. In addition, for creating this prediction model, we followed the TRIPOD checklist (Supplementary Material S1).

Patient Cohort

This retrospective study included patients diagnosed with RVO-ME at the Department of Ophthalmology, the Second Xiangya Hospital of Central South University, between June 2018 and May 2024. The medical records of eligible patients were collected retrospectively from the electronic medical record system. Inclusion criteria were as follows: age greater than 18 years, visual impairment related to RVO-ME, and a macular central subfield thickness (CST) of 250 µm or more. CST was determined as the average thickness between the internal limiting membrane and Bruch's membrane within a 1-mm diameter centered on the macula of the Early Treatment Diabetic Retinopathy Study (ETDRS) grid; the receipt of at least one anti-VEGF intravitreal injection, including ranibizumab 0.5 mg/0.05 mL (Novartis Pharma AG, Basel, Switzerland), aflibercept 2.0 mg/0.05 mL (Bayer Healthcare Pharmaceuticals, Berlin, Germany), or conbercept 0.5 mg/0.05 mL (Kanghong Biotech Co., Ltd., Chengdu, China); and active follow-up before and during the administration of at least the first intravitreal injection. The exclusion criteria encompassed visual impairment caused by other ocular diseases, such as severe cataract, glaucoma, age-related macular degeneration, diabetic ME, vitreomacular traction, or uveitis. Additionally, participants who switched to intravitreal steroids or underwent vitreoretinal surgery, as well as those with missing follow-up information or poor-quality medical images, were excluded. According to prior research,[15,16] the definition of limit early responder (LER) encompassed a reduction in CST of less than 10%, a gain in best-corrected visual acuity (BCVA) of less than 5 ETDRS letters, or both, at the 1-month time point after the first injection. Early responder (ER) was defined as a reduction in CST of more than 10%, a gain in BCVA of more than 5 ETDRS letters, or both. Ocular samples were randomly allocated into training and test sets at a 7:3 ratio.

External Validation

An external dataset consisting of patients with RVO-ME from the Second Xiangya Hospital, Central South University, spanning from June 2024 to December 2024, was used for external validation. The inclusion and exclusion criteria were identical to those of the derivation cohort.

Imaging Acquisition and Region of Interest Segmentation

This study also used the concept of "OCT-omics" developed by our team,[17] which was introduced as a novel approach to extract, select, and analyze high-throughput quantitative features from OCT images, thereby aiming to give a complete representation of the retina in diseases with a large number of features.

Spectral-domain OCT images were obtained using the Optovue RTVue XR Avanti system (Optovue Inc., Fremont, CA, USA) for all eyes included in this study. Follow-up assessments involved radial scans (6 × 6 mm) centered on the fovea. Region of interest (ROI) segmentation and feature extraction were conducted on DICOM-formatted B-scan OCT images along the vertical meridian.

The process of manually segmenting the retinal layers, spanning from the inner limiting membrane to the Bruch's membrane, was conducted utilizing the 3D Slicer software (version 5.0.3, https://www.slicer.org/). Two ophthalmologists (author J.Q., with 4 years of experience, and author B.C., also with 4 years of experience) independently performed the segmentation, unaware of the patient groups or treatment outcomes, thereby ensuring objectivity and minimizing bias. Subsequently, a senior retina specialist (author J.L., with 30 years of experience) reviewed and confirmed the segmentation results.

Radiomics Feature Extraction and Selection

Radiomics features were extracted from the segmented images utilizing the Pyradiomics module within the 3D Slicer software platform.[18] The OCT images were resampled to voxel dimensions of 1 × 1 × 1 mm, with a bin width value of 25.0. The extracted features comprised eight distinct classes, namely first-order statistics, Gray Level Co-occurrence Matrix (GLCM), Gray Level Run Length Matrix (GLRLM), Gray Level Size Zone Matrix (GLSZM), Neighboring Gray Tone Difference Matrix (NGTDM), and Gray Level Dependence Matrix (GLDM), 2D shape, and wavelet-based features. These feature classes collectively encompassed a comprehensive array of quantitative information pertaining to intensity, shape, texture, and spatial relationships within the OCT images.

In order to maintain consistency, the standardization of features was conducted through z-score transformation. The interobserver reproducibility of the ROI and radiomic feature extraction were assessed by 2 ophthalmologists in a blinded manner, utilizing the intraclass correlation coefficient (ICC) on a sample of 15 randomly selected eyes. Features exhibiting ICC values exceeding 0.75 were deemed to possess favorable reproducibility. Subsequently, to further exclude the effect of anti-VEGF agent type on outcomes, dummy variables were created for categorical agent types. Following this feature, the importance in random forest and Recursive Feature Elimination (RFE)

Investigative Ophthalmology & Visual Science

methods were used to select these screened OCT-omics features, alongside the dummy variables representing drug types.

Development and Validation of Prediction Models

In this study, two machine learning models, namely support vector machine (SVM) and back propagation neural network (BPNN) were developed and trained using the selected OCT-omics features. The SVM model used a linear kernel function with a C value of 1 and a maximum of 1000 iterations. On the other hand, the BPNN model utilized a single hidden layer consisting of 100 neurons and employed the hyperbolic tangent function (tanh) as the activation function. The Limited-memory Broyden–Fletcher–Goldfarb–Shanno (LBFGS) solver was used, along with an L2 regularization term of 1. Both models underwent training using five-fold cross-validation. This study evaluated the classification performances and generalization abilities of three classifiers, namely logistic regression, SVM, and BPNN. Performance metrics, such as accuracy, sensitivity, specificity, precision, negative predictive value, and F1 score, were computed for the training, test, and external validation sets. To assess the classifier performance, confusion matrices and receiver operating characteristic (ROC) curves along with their corresponding area under the curve (AUC) values were used by utilizing the R packages *ggplot2*, *reshape2*, and *pROC*.

Establishment of OCT-Omics Models

The construction of the logistic regression model took place in the training set, and subsequent computation of the OCT-omics score was conducted for each sample. The OCT-omics score is calculated from the results of the logistic regression model via a sigmoid function. To compare OCT-omics scores between the LER and ER groups, the Mann-Whitney *U* test was utilized. Additionally, Spearman correlation analysis was performed to examine the correlation between OCT-omics scores and change rate of CST after treatment. Change rate of CST is equal to the ratio of the difference between the CST of pretreatment and post-treatment to the CST of pretreatment (change rate of CST = $(CST_{pre\text{-}treatment}\text{-}CST_{post\text{-}treatment})/CST_{pre\text{-}treatment}$). The assessment of clinical utility involved the decision curve analysis (DCA), with net benefits quantified using the rmda R package.

Statistical Analysis

The statistical analyses were performed utilizing R software (version 4.4.1) and the SPSSPRO online data analysis platform (https://www.spsspro.com). Descriptive statistics for continuous variables included means ± standard deviations (SDs) or medians with interquartile ranges (IQRs). Categorical variables were expressed as counts and percentages. Independent *t*-tests or Mann-Whitney *U* tests were used for comparing continuous variables between groups, depending on the normality of the data. Spearman correlation analysis was utilized to examine correlations among continuous variables. All tests were 2-sided, with P values < 0.05 considered statistically significant.

Results

Patient Characteristics and Data Distribution

The study process involved a sequential flow, as depicted in Figure 1. A total of 307 patients diagnosed with RVO-ME were registered in the cohort during the study period. After excluding 155 patients without available OCT images, 153 eyes from 152 patients were included in the final study. In addition, 82 eyes from 81 patients were included in the external validation set. Table 1 shows the clinical characteristics of the patients in the training set ($n = 106$), the test set ($n = 46$), and the external validation set ($n = 81$). Among 233 patients, 122 (52.36%) were male, 111 (47.64%) were female ($p = 0.251$), and the mean age was 60 years (SD = 13, $P = 0.486$). No significant differences of the distribution of the initial three medication types were observed among the training, test, and external validation sets ($P = 0.783$).

Machine Learning Models Development and Clinical Implication Evaluation

A total of 837 quantitative features were extracted using the 3D slicer software platform, of which 617 features with ICC values exceeding 0.75 were retained. Dummy variables were integrated to represent the presence of different drug types. After using the random forest method and RFE algorithm, the remaining eight features were used to establish the radiomics signature. The comprehensive feature screening procedure is presented in Supplementary Material S2. Among six classifier models evaluated, we selected two classifiers for further analysis: SVM and BPNN.

The OCT-omics classification models (BPNN, SVM, and logistic) demonstrated strong discriminative performance in all sets. As shown in Figure 2, in the training set, the AUC values of the logistic regression model, the BPNN model, and the SVM model were 0.977, 0.916, and 0.919, respectively, whereas in the test set, they were 0.912, 0.882, and 0.914, respectively. Notably, in the external validation set, all classifiers maintained strong performance. The BPNN classifier exhibited a sensitivity of 0.915, a specificity of 0.783, an F1 score of 0.915, and an AUC of 0.804. The SVM classifier showed a sensitivity of 0.932, a specificity of 0.739, an F1 score of 0.917, and an AUC of 0.802. The logistic classifier achieved a sensitivity of 0.864, a specificity of 0.696, an F1 score of 0.872, and an AUC of 0.794. The results are summarized in Table 2.

Development of OCT-Omics Model and Evaluation of Clinical Application

The OCT-omics model was provided below: "Y = 2.378-1.56*originalglszmLowGrayLevelZoneEmphasis-2.175*wavelet-HLHglrlmRunVariance+1.557*wavelet-HLHglszmZoneVariance+1.598*wavelet-HHHglcmMaximumProbability-2.977*wavelet-HHHglrlmRunEntropy-6.34*wavelet-HHHglrlmRunLengthNonUniformityNormalized-1.764*wavelet-HHHglszmLowGrayLevelZoneEmphasis-1.129*wavelet-LLLfirstorderMinimum (Fig. 3a)". The OCT-omics scores were significantly higher in the ER group compared to the LER group in both the training set ($P = 1.9e\text{-}11$) and the test set ($P = 3.2e\text{-}06$; Fig. 3b). Spearman correlation analysis showed a significant positive correlation between OCT-omics scores and the change rate of CST after treatment in the training

Investigative Ophthalmology & Visual Science

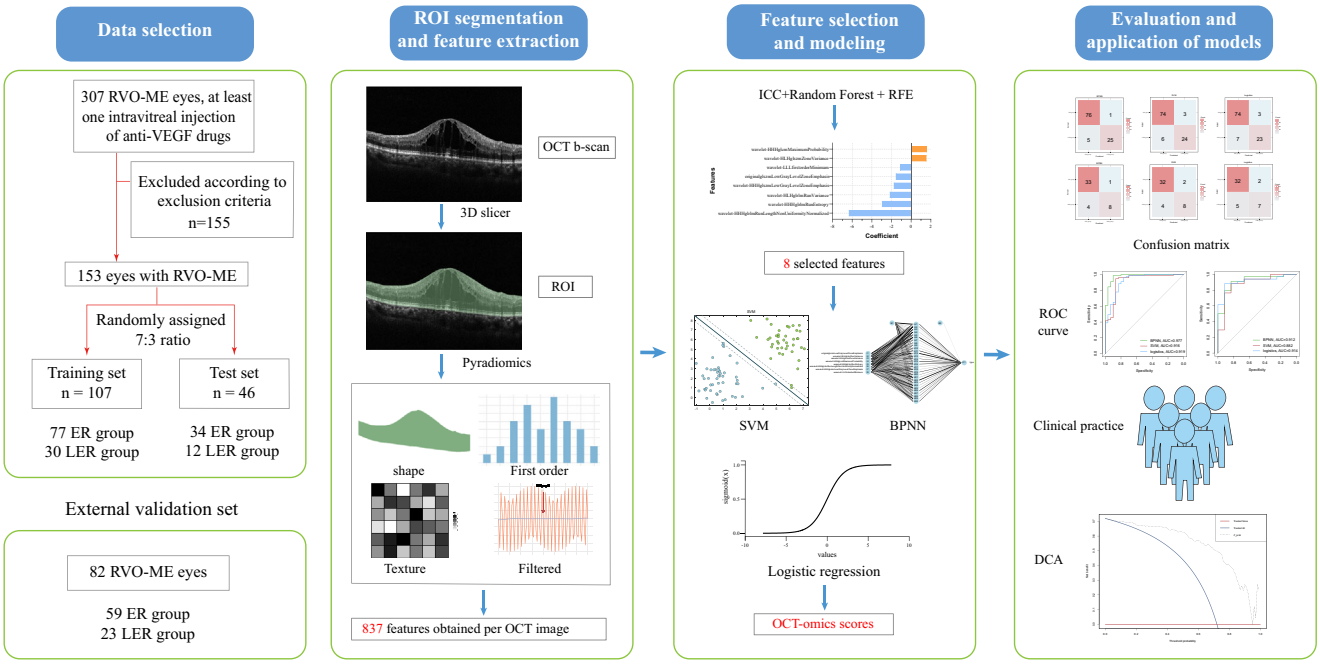

Figure 1. The flowchart for the study.

Table 1. Clinical Characteristics of the Total Subjects, Training Set, Test Set, and External Validation Set

	N (%)/Mean ± SD				
Characteristic	**Total**	**Training Set**	**Test Set**	**External Validation**	***P* Value**
Participant level	**(*n* = 233)**	**(*n* = 106)**	**(*n* = 46)**	**(*n* = 81)**	
Sex					0.251
Male (%)	122 (52.36)	54 (50.94)	29 (63.04)	39 (48.15)	
Female (%)	111 (47.64)	52 (49.06)	17 (36.96)	42 (51.85)	
Age, y, M (SD)	60 (13)	58 (13)	61 (12)	62 (13)	0.486
Eye level	**(*n* = 235)**	**(*n* = 107)**	**(*n* = 46)**	**(*n* = 82)**	
Laterality					0.398
Right (%)	118 (50.21)	50 (46.73)	27 (58.70)	41 (50.00)	
Left (%)	117 (49.79)	57 (53.27)	19 (41.30)	41 (50.00)	
CST, mm					
Pre-therapy, M (SD)	450 (181)	475 (170)	450 (227)	418 (158)	0.094
Post-therapy, M (SD)	314 (128)	320 (131)	334 (155)	294 (101)	0.197
Anti-VEGF drug					0.783
Ranibizumab (%)	148 (62.98)	79 (73.83)	30 (65.22)	61 (47.56)	
Conbercept (%)	72 (30.64)	19 (17.76)	12 (26.09)	15 (50.00)	
Aflibercept (%)	15 (6.38)	9 (8.41)	4 (8.69)	6 (2.44)	
RVO types					0.389
CRVO (%)	100 (42.55)	41 (38.32)	23 (50.00)	36 (43.90)	
BRVO (%)	135 (57.45)	66 (61.68)	23 (50.00)	46 (56.10)	

Mean ± standard deviations (SDs) were reported for quantitative variables, and number (percentage) was reported for categorical variables.

set, the test set, and the external validation set (R = 0.62, P < 2.2e-16; R = 0.5, P = 0.00051; and R = 0.43, P = 6.5e−05; Fig. 3c). The DCA of the three sets showed that the OCT-omics models had improved clinical utility overall, as evidenced by the curve shapes (Figure 3d).

Clinical Significance of the OCT-Omics Models

Figure 4 illustrates the short- and long-term prognostic effects of two typical cases in this study, along with the predictive performance of anti-VEGF therapy in the OCT-omics model group. Figure 4a presents a 65-year-old female patient with an initial CST of 677 µm and an OCT-omics score of 10.58. The BPNN model and the SVM model both predicted a high probability of ER (99%), indicating a favorable response to the treatment. CST gradually decreased to 468 µm after the first injection, 365 µm after 3 injections, and 189 µm after 5 injections. Figure 4b shows an 84-year-old male patient with an OCT-omics score of −4.26. The probability of ER predicted by the BPNN model is 1%, whereas the SVM model predicts a 10% probability for ER. The subsequent long-term prognosis also proves that the patient is LER

Investigative Ophthalmology & Visual Science

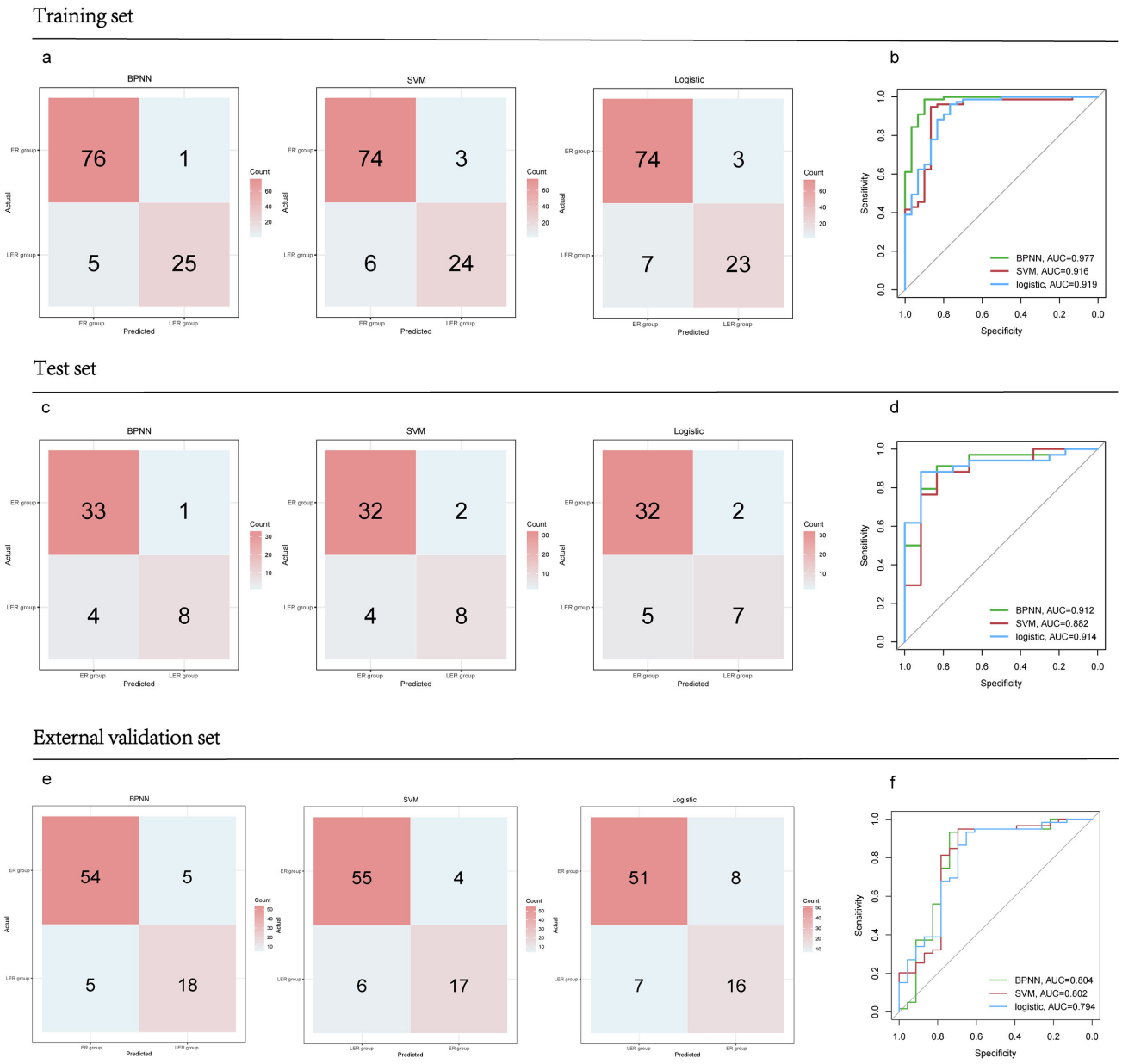

Figure 2. Confusion matrices of the BPNN model, the SVM model and the logistic regression model in the training set (**a**), the test set (**c**), and the external validation (**e**) set. ROC analysis showing that the performance of the BPNN model (*green line*), the SVM model (*red line*), and the logistic regression (*blue line*) in the training (**b**), the test (**d**), and the external validation (**f**) cohorts.

Table 2. Detail Performances of Machine Models

	Training Set			Test Set			External Validation Set		
	BPNN	**SVM**	**Logistic**	**BPNN**	**SVM**	**Logistic**	**BPNN**	**SVM**	**Logistic**
ACC	0.944	0.916	0.907	0.891	0.870	0.848	0.878	0.878	0.817
SEN	0.987	0.961	0.961	0.971	0.941	0.941	0.915	0.932	0.864
SPE	0.833	0.800	0.767	0.667	0.667	0.583	0.783	0.739	0.696
PRE	0.938	0.925	0.914	0.892	0.889	0.865	0.915	0.902	0.879
NPV	0.962	0.889	0.885	0.889	0.800	0.778	0.783	0.810	0.667
F1 score	0.962	0.943	0.937	0.930	0.914	0.901	0.915	0.917	0.872

Investigative Ophthalmology & Visual Science

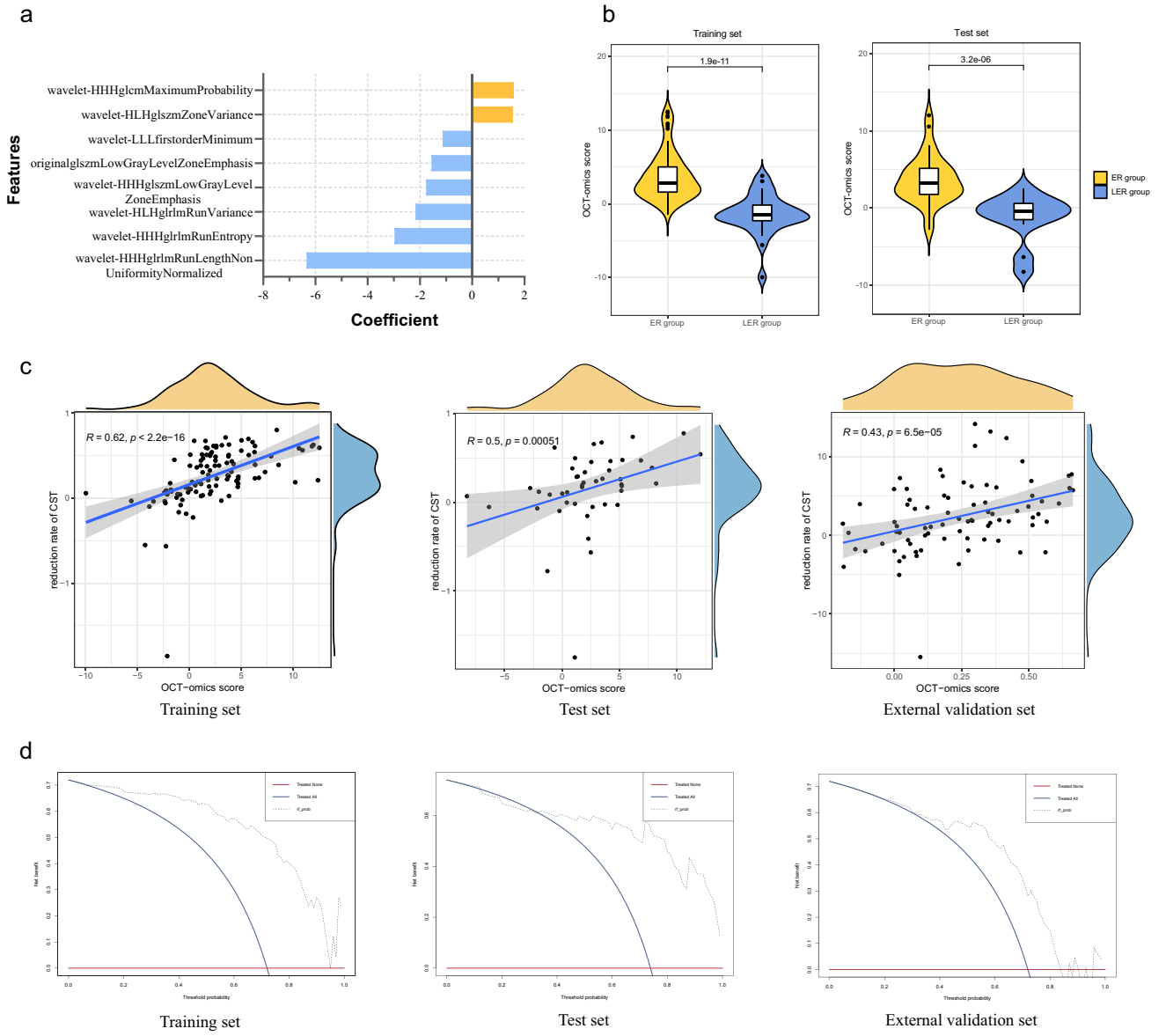

Figure 3. (**a**) The distribution of coefficients for the eight features in the logistic regression model. (**b**) Violin plots comparing OCT-omics scores between ER and LER groups in the training and test sets. (**c**) Scatterplot illustrating the correlation between OCT-omics score and rate of CST reduction after treatment in the training, the test, and the external validation sets. (**d**) Decision curve analysis curves of the OCT-omics model in the training, the test, and the external validation sets.

after anti-VEGF treatment. The initial CST is 486 µm, the CST after 1 injection is 500 µm, the CST after 3 injections are 551 µm, and the CST after 5 injections are 502 µm.

Discussion

Herein, we present and evaluated OCT-based radiomics models for predicting the efficacy of anti-VEGF therapy in patients with RVO-ME. The model demonstrated outstanding predictive performance among the training, the test, and the external validation sets, potentially offering advantages to patients in terms of personalized medication selection, thereby significantly enhancing cost-effectiveness and visual prognosis. Furthermore, the newly introduced OCT-omics score exhibits a moderate correlation with the rate of change in CST, thereby facilitating ophthalmologists in predicting treatment outcomes for patients more intuitively and conveniently.

The first-line treatment for RVO-ME is anti-VEGF therapy.[4] Nonetheless, some patients still suffer from refractory edema after intraocular injection.[3] Patients with RVO-ME who exhibit favorable early responses to anti-VEGF therapy are anticipated to experience enhanced visual function restoration and reduced long-term treatment burden.[19] Therefore, it is crucial to differentiate these patients. The feasibility of assessing efficacy of 1 month after single anti-VEGF therapy has been demonstrated by a study showing that a 25% decrease in central retinal thickness (CRT) 1 month after single anti-VEGF therapy is effective in differentiating between responders and nonresponders to anti-VEGF medications.[20] In summary, we are trying to investigate the feasibility of utilizing preoperative examinations

Investigative Ophthalmology & Visual Science

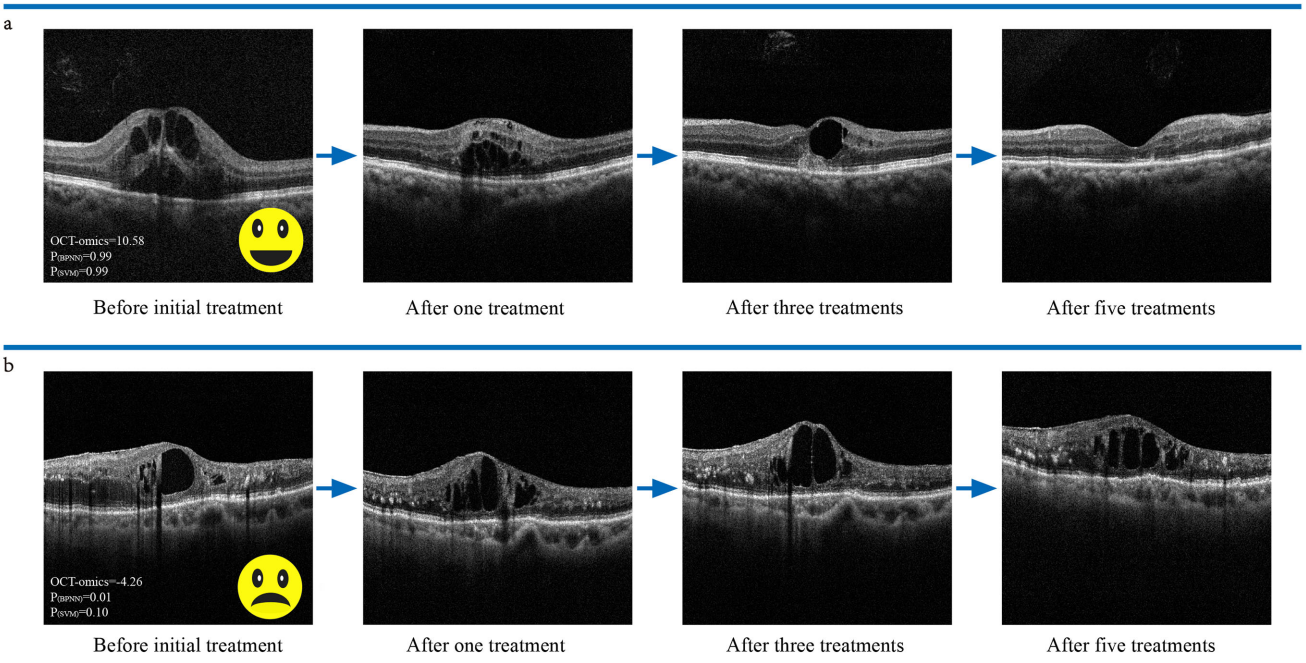

Figure 4. (**a**) Long-term status of RVO of one patient in the ER group. (**b**) Long-term status of RVO of one patient in the LER group.

to predict the effect of a single anti-VEGF drug injection in patients with RVO-ME and to provide timely and individualized medication guidance to patients.

Intraocular pre-injection and follow-up evaluation of RVO-ME can be effectively conducted using OCT, which is considered the most reliable noninvasive test.[4] There are several OCT predictors of RVO-ME, including the external limiting membrane, ellipsoid zone, hyper-reflective foci, small macular cysts, central macular thickness (CMT) or central foveal thickness (CFT) reduction rate, widefield retinal thickness map, choroidal thickness, and choroidal vascularity index (CVI)[19,21–23] as well as several other ocular imaging markers,[22,24–26] which can be linked to alterations in retinal structure to provide insight into the prediction. Additionally, there are also systemic markers that can predict the outcome of patients with RVO-ME following anti-VEGF treatment,[22,27–29] which can establish a correlation between RVO and systemic pathology. However, RVO is a multifactorial disease, and if a single prognosis factor, such as baseline choroidal thickness obtained from OCT is considered, it only provides information on a specific aspect while disregarding other contributing factors.[30] The utilization of singular indicators to forecast treatment outcomes remains precarious, and the current trend involves constructing predictive models based on multiple indicators.

Machine learning methods have been used to analyze distinct retinal structures in OCT images and clinical data, yielding favorable predictive outcomes for the efficacy of anti-VEGF therapy.[15,31,32] Additionally, several studies have conducted multimetric predictive modeling, with one example being a longitudinal mixed effects model that incorporates OCT imaging fluid factors and clinical data to predict the BCVA of patients 1 year after anti-VEGF treatment.[33] However, in their machine learning model, the OCT-omics data component focused only on the volume of intraretinal and subretinal fluid, while neglecting other traditional imaging markers in SD-OCT images that could impact the prediction of anti-VEGF efficacy. The generative adversarial network has the capability to generate virtual predictive OCT images that closely resemble the real images after 1 month of anti-VEGF treatment, using pretreatment OCT images.[34] Although this method does not require feature extraction for machine learning or modality fusion, its main limitation lies in the lack of long-term predictions and the interpretability of the output images. Our study introduces a novel approach wherein we comprehensively extract and analyze features of the complete OCT image rather than single traditional imaging marker prior to treatment, and subsequently use these features to construct a prediction model by the machine learning theory, which saves time and labor costs and uses minimal clinical information to prognose.

The study is subject to certain limitations. First, it was a retrospective study conducted at a solitary institution, and future researches will involve larger sample sizes through multicenter prospective studies. Second, due to the limited sample size in each subgroup, this study only analyzed the distribution of each subgroup in the training, testing, and validation sets without considering the establishment of OCT-omics models for prediction based on each subgroup, such as the CRVO and BRVO subgroups, or drug-based subgroups (aflibercept, conbercept, and ranibizumab). Furthermore, the manual segmentation method reduced the automation of our model. The next step will be to seek multidisciplinary collaboration to develop more accurate automated segmentation methods. Nevertheless, we assert the value of the OCT radiomics approach due to its noninvasive nature and the absence of a need for patients to undergo supplementary tests in order to predict treatment outcomes. Moreover, the utilization of radiomics-based analysis furnishes ophthalmologists with a greater wealth of imaging information without the need to acquire new interpretation expertise of OCT.

In conclusion, we have successfully devised and evaluated an OCT-based retinal imaging model aimed at prognos-

Investigative Ophthalmology & Visual Science

ticating anti-VEGF therapeutic responses for RVO-ME. The OCT radiomics approach will provide valuable information and help with precision medicine without additional healthcare costs and invasive tests.

Acknowledgments

Supported by Changsha Municipal Natural Science Foundation (kp2208325).

Disclosure: **B. Chen**, None; **J. Qiu**, None; **Y. Meng**, None; **Y. Liang**, None; **D. Liu**, None; **Y. Hu**, None; **Z. Meng**, None; **J. Luo**, None

References

1. Song P, Xu Y, Zha M, Zhang Y, Rudan I. Global epidemiology of retinal vein occlusion: a systematic review and meta-analysis of prevalence, incidence, and risk factors. *J Glob Health*. 2019;9(1):010427.
2. Hayreh SS. Photocoagulation for retinal vein occlusion. *Prog Retin Eye Res*. 2021;85:100964.
3. Noma H, Yasuda K, Shimura M. Cytokines and pathogenesis of central retinal vein occlusion. *J Clin Med*. 2020;9(11):3457.
4. Schmidt-Erfurth U, Garcia-Arumi J, Gerendas BS, et al. Guidelines for the management of retinal vein occlusion by the European Society of Retina Specialists (EURETINA). *Ophthalmologica*. 2019;242(3):123–162.
5. Ang JL, Ah-Moye S, Kim LN, et al. A systematic review of real-world evidence of the management of macular oedema secondary to branch retinal vein occlusion. *Eye (Lond)*. 2020;34(10):1770–1796.
6. Wallsh JO, Gallemore RP. Anti-VEGF-resistant retinal diseases: a review of the latest treatment options. *Cells*. 2021;10(5):1049.
7. Castro-Navarro V, Monferrer-Adsuara C, Navarro-Palop C, Montero-Hernández J, Cervera-Taulet E. Optical coherence tomography biomarkers in patients with macular edema secondary to retinal vein occlusion treated with dexamethasone implant. *BMC Ophthalmol*. 2022;22(1):191.
8. Mo B, Zhou HY, Jiao X, Zhang F. Evaluation of hyperreflective foci as a prognostic factor of visual outcome in retinal vein occlusion. *Int J Ophthalmol*. 2017;10(4):605–612.
9. Ip M, Hendrick A. Retinal vein occlusion review. *Asia Pac J Ophthalmol (Phila)*. 2018;7(1):40–45.
10. Song S, Yu X, Zhang P, Dai H. Changes in macular microvascular structure in macular edema secondary to branch retinal vein occlusion treated with antivascular endothelial growth factor for one year. *J Ophthalmol*. 2021;2021:6645452.
11. Lambin P, Leijenaar RTH, Deist TM, et al. Radiomics: the bridge between medical imaging and personalized medicine. *Nat Rev Clin Oncol*. 2017;14(12):749–762.
12. Zhang M, Tong E, Wong S, et al. Machine learning approach to differentiation of peripheral schwannomas and neurofibromas: a multi-center study. *Neuro Oncol*. 2022;24(4):601–609.
13. Jiang YW, Xu XJ, Wang R, Chen CM. Radiomics analysis based on lumbar spine CT to detect osteoporosis. *Eur Radiol*. 2022;32(11):8019–8026.
14. Gallardo M, Munk MR, Kurmann T, et al. Machine learning can predict anti-VEGF treatment demand in a treat-and-extend regimen for patients with neovascular AMD, DME, and RVO associated macular edema. *Ophthalmol Retina*. 2021;5(7):604–624.
15. Kailar RS, Perkins SW, Kuo BL, Singh RP. Characterizing and predicting limited early response in eyes with retinal vein occlusion using machine learning in routine clinical practice. *Ophthalmic Surg Lasers Imaging Retina*. 2023;54(4):231–237.
16. Roy R, Saurabh K, Ghose A, et al. Quantitative reduction in central foveal thickness after first anti-VEGF injection as a predictor of final outcome in BRVO patients. *Asia Pac J Ophthalmol (Phila)*. 2017;6(3):261–265.
17. Meng Z, Chen Y, Li H, et al. Machine learning and optical coherence tomography-derived radiomics analysis to predict persistent diabetic macular edema in patients undergoing anti-VEGF intravitreal therapy. *J Transl Med*. 2024;22(1):358.
18. van Griethuysen JJM, Fedorov A, Parmar C, et al. Computational radiomics system to decode the radiographic phenotype. *Cancer Res*. 2017;77(21):e104–e107.
19. Zhou J, Ma H, Zhou X, et al. Two-week central macular thickness reduction rate >37% predicts the long-term efficacy of anti-vascular endothelial growth factor treatment for macular edema secondary to retinal vein occlusion. *Front Med (Lausanne)*. 2022;9:851238.
20. Wolfe JD, Shah AR, Yonekawa Y, et al. Receiver operating characteristic curve to predict anti-VEGF resistance in retinal vein occlusions and efficacy of Ozurdex. *Eur J Ophthalmol*. 2016;26(2):168–173.
21. Park HM, Kim YH, Lee BR, Ahn SJ. Topographic patterns of retinal edema in eyes with branch retinal vein occlusion and their association with macular edema recurrence. *Sci Rep*. 2021;11(1):23249.
22. Chatziralli I, Kazantzis D, Kroupis C, et al. The impact of laboratory findings and optical coherence tomography biomarkers on response to intravitreal anti-VEGF treatment in patients with retinal vein occlusion. *Int Ophthalmol*. 2022;42(11):3449–3457.
23. Hwang BE, Kim M, Park YH. Role of the choroidal vascularity index in branch retinal vein occlusion (BRVO) with macular edema. *PLoS One*. 2021;16(10):e0258728.
24. Huang PW, Lai CC, Hwang YS, et al. Treatment responses for branch retinal vein occlusion predicted by semi-automated fluorescein angiography quantification. *BMC Ophthalmol*. 2022;22(1):50.
25. Takei T, Nagai N, Ohkoshi K, Ozawa Y. Arm-to-retina time predicts visual outcome of anti-vascular endothelial growth factor treatment for macular edema due to central retinal vein occlusion. *Sci Rep*. 2022;12(1):2194.
26. Tang W, Liu W, Guo J, et al. Wide-field swept-source OCT angiography of the periarterial capillary-free zone before and after anti-VEGF therapy for branch retinal vein occlusion. *Eye Vis (Lond)*. 2022;9(1):25.
27. Rao J, Wu N, Qu X, et al. The role of serum inflammation-based factors in anti-vascular endothelial growth factor treatment for macular edema secondary to retinal vein occlusion and its subtypes. *Ophthalmic Res*. 2021;64(2):237–245.
28. Liu X, Xie C, Wang Y, Xu Y, Zhu S, Fang Y. A retrospective study assessing the factors associated with visual outcome in retinal vein occlusion patients after anti-VEGF therapy. *PeerJ*. 2021;9:e12599.
29. Tomita R, Iwase T, Goto K, Yamamoto K, Ra E, Terasaki H. Correlation between macular vessel density and number of intravitreal anti-VEGF agents for macular edema associated with branch retinal vein occlusion. *Sci Rep*. 2019;9(1):16388.
30. Rayess N, Rahimy E, Ying GS, et al. Baseline choroidal thickness as a predictor for treatment outcomes in central retinal vein occlusion. *Am J Ophthalmol*. 2016;171:47–52.

31. Matsui Y, Imamura K, Chujo S, et al. Which explanatory variables contribute to the classification of good visual acuity over time in patients with branch retinal vein occlusion with macular edema using machine learning? *J Clin Med*. 2022;11(13):3903.
32. Matsui Y, Imamura K, Ooka M, et al. Classification of good visual acuity over time in patients with branch retinal vein occlusion with macular edema using support vector machine. *Graefes Arch Clin Exp Ophthalmol*. 2022;260(5):1501–1508.
33. Vogl WD, Waldstein SM, Gerendas BS, Schlegl T, Langs G, Schmidt-Erfurth U. Analyzing and predicting visual acuity outcomes of anti-VEGF therapy by a longitudinal mixed effects model of imaging and clinical data. *Invest Ophthalmol Vis Sci*. 2017;58(10):4173–4181.
34. Xu F, Yu X, Gao Y, et al. Predicting OCT images of short-term response to anti-VEGF treatment for retinal vein occlusion using generative adversarial network. *Front Bioeng Biotechnol*. 2022;10:914964.